

See discussions, stats, and author profiles for this publication at: <https://www.researchgate.net/publication/260218467>

# 4,4'-Diaminodiphenyl ether derivatives: Synthesis, spectral, optical, thermal characterization and in-vitro cytotoxicity against Hep 3B and IMR 32 human cell lines

ARTICLE *in* EUROPEAN JOURNAL OF MEDICINAL CHEMISTRY · JANUARY 2014

Impact Factor: 3.45 · DOI: 10.1016/j.ejmech.2013.12.035 · Source: PubMed

---

CITATIONS

3

---

READS

29

3 AUTHORS, INCLUDING:



Vinay Kumar Singh

The Maharaja Sayajirao University of Baroda

23 PUBLICATIONS 120 CITATIONS

SEE PROFILE



This article appeared in a journal published by Elsevier. The attached copy is furnished to the author for internal non-commercial research and education use, including for instruction at the authors institution and sharing with colleagues.

Other uses, including reproduction and distribution, or selling or licensing copies, or posting to personal, institutional or third party websites are prohibited.

In most cases authors are permitted to post their version of the article (e.g. in Word or Tex form) to their personal website or institutional repository. Authors requiring further information regarding Elsevier's archiving and manuscript policies are encouraged to visit:

<http://www.elsevier.com/authorsrights>



Contents lists available at ScienceDirect

## European Journal of Medicinal Chemistry

journal homepage: <http://www.elsevier.com/locate/ejmech>

## Original article

4,4'-Diaminodiphenyl ether derivatives: Synthesis, spectral, optical, thermal characterization and *in-vitro* cytotoxicity against Hep 3B and IMR 32 human cell linesVinay K. Singh<sup>a,\*</sup>, Rahul Kadu<sup>a</sup>, Hetal Roy<sup>b</sup><sup>a</sup> Department of Chemistry, Faculty of Science, The Maharaja Sayajirao University of Baroda, Vadodra 390 002, Gujarat, India<sup>b</sup> Department of Zoology, Faculty of Science, The Maharaja Sayajirao University of Baroda, Vadodra 390 002, India

## ARTICLE INFO

## Article history:

Received 2 November 2013

Received in revised form

21 December 2013

Accepted 24 December 2013

Available online 6 January 2014

## Keywords:

4,4'-Diaminodiphenyl ether derivatives

Cytotoxic activity

MTT assay

Optical properties

## ABSTRACT

4,4'-Diaminodiphenyl ether was selected as a lead compound to prepare a novel series of bisimine derivatives bearing polyaromatic hydrocarbon substituents and their reduced benzyl forms. The new compounds were structurally characterized by microanalysis, mass, IR, <sup>1</sup>H, <sup>13</sup>C, DEPT-135, HSQC, g-COSY NMR spectroscopy, UV–visible, fluorescence spectrophotometers and by thermogravimetric analysis. The antitumor activity of these derivatives was evaluated *in-vitro* against Hep 3B and IMR 32 by the MTT assay and the results were compared with cisplatin. Interestingly, some compounds were found extremely active against both the cell lines and proved to be more potent as cytotoxic agents than cisplatin. Morphological evidences suggest the induction of apoptosis and explain the mode of action of these derivatives as antitumor agents.

© 2014 Elsevier Masson SAS. All rights reserved.

## 1. Introduction

Interest in the search of novel potent anticancer compounds has been continued because chemotherapy used for the cancer sufferers always shows some undesirable side effects. Thus identification of new molecules that induce apoptosis i.e. nuclear condensation and DNA fragmentation by different biological as well as cytological processes is essential for the discovery and development of novel anticancer agents [1,2].

The polyaromatic hydrocarbons have been considered as one of the robust antitumor agents. For instance the biological evaluations of polyaromatic compounds such as chrysene and 1-pyrene methylamine derivatives have been reported by Becker and co-workers [3–5]. These compounds have been shown to possess a broad spectrum of chemotherapeutic activity against both murine and human tumors and in some case these were chosen for clinical development. Recently, a new class of compounds has been reported [6] as polyaromatic substituted podophyllotoxin congeners [7]. These have been proven promising structures for the development of new anticancer agents for human cancer cell lines. It appears that O-linked (ethers, esters) and S-linked (thioethers)

compounds are less active in comparison to the N-linked congeners [1,8–11].

Although a primary investigation on *in-vivo* mutagenicity of 4,4'-diaminodiphenyl ether and its N-acetyl derivative towards *Salmonella typhimurium* TA98 and TA100 was reported in 1985 by Tanaka et al. [12], there is no reports on further investigations of biological properties of 4,4'-diaminodiphenyl ether and its derivatives. Moreover, no data are available to assess the mutagenicity or teratogenicity of any derivative of 4,4'-diaminodiphenyl ether to human. Thus it was pertinent to derivatize 4,4'-diaminodiphenyl ether and explore the potential uses of these functional molecules from the biological and medicinal points of view. Pharmaceutical development for lower cost of production of generic and proprietary products using large-scale syntheses brings a new challenge in the present era. Thus, the ease of synthesis and interesting *in-vitro* anticancer activity against human Hep 3B (hepatoma) and IMR 32 (neuroblastoma) cell lines, make the present series of bisimine and diamine derivatives of 4,4'-diaminodiphenyl ether bearing polyaromatic hydrocarbon substituents as a promising new structures (Chart 1) for the development of new anticancer agents. Apart from this, the presence of imine (–C=N–) functionality in conjugation with polyaromatic substituents, increases the extended  $\pi$ -electron delocalization in the organic framework and thus alters the electronic and optical properties of these compounds.

\* Corresponding author.

E-mail address: [vks.msu@gmail.com](mailto:vks.msu@gmail.com) (V.K. Singh).

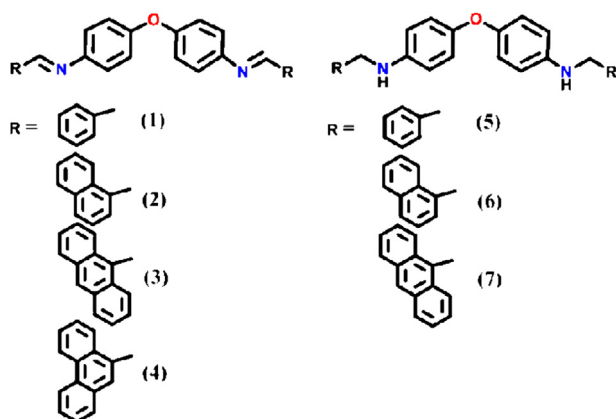


**Chart 1.** Generic structures of bisimine and diamine derivatives bearing polyaromatic hydrocarbon substituents.

## 2. Results and discussion

### 2.1. Synthesis and characterization of the compounds

Bisimine derivatives 4,4'-bis(arylmethylideneamino)diphenyl ethers **1–4** were obtained in >80% yield by condensation of 4,4'-diaminodiphenyl ether with different aromatic aldehydes (Scheme 1). Practically, the reaction mixtures were refluxed in toluene containing a catalytic amount of glacial acetic acid by using a Dean–Stark apparatus. Dean–Stark apparatus was helpful in removing H<sub>2</sub>O molecules formed during the course of the reaction as azeotropic mixture and thereby shifts the equilibrium towards a product, with higher yield and in less time. This synthetic method was found to be superior over a number of reported methods which are time consuming and produce relatively low yields. Diamine derivatives 4,4'-bis(arylmethylamino)diphenyl ethers **6** and **7** were synthesized by reduction of corresponding bisimines with NaBH<sub>4</sub> in ethanol in good yield. The synthesis of **1** and **5** has been recently reported by us [13] whereas compound **3** is prepared by a modified literature procedure [14]. The reductive amination strategy used for the reduction of these bisimine compounds is found to be superior over several conventional procedures [15].

The new compounds were characterized by elemental analysis, mass spectroscopy, IR, UV–visible, NMR (<sup>1</sup>H, <sup>13</sup>C, DEPT-135) and 2D NMR (gCOSY, HSQC) spectroscopy. These compounds were further analyzed for their optical behaviors by using UV–visible absorption, emission and transmittance measurements. The elemental analysis data for **2–4** and **6, 7** are in good agreement with their compositions. The infrared, NMR and UV–visible spectra of these compounds are consistent with their chemical formula determined by elemental analysis and further confirmed by mass spectral analysis. The characterization data of the newly synthesized compounds are summarized in Tables 1–3.

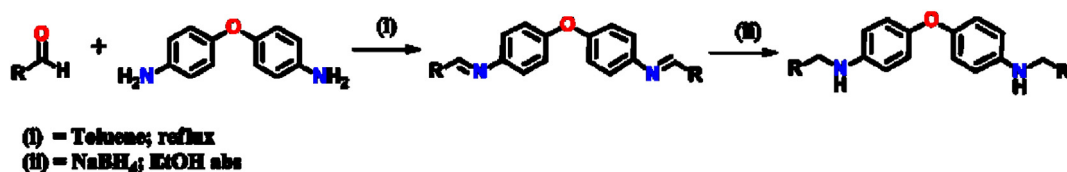
In the IR spectrum of bisimines **2–4** (Table 1), the most characteristic band appeared in the region of 1664–1617 cm<sup>−1</sup>, is due to

$\nu(\text{C}=\text{N})$  whereas diamines **6** and **7** displayed  $\nu(\text{N}—\text{H})$  bands at 3373 and 3389 cm<sup>−1</sup> respectively. All the compounds showed a weak intensity bands in the regions of 3012–2830 cm<sup>−1</sup> due to the aromatic, benzyldiene and benzyl  $\nu(\text{C}—\text{H})$  stretching vibrations respectively. The appearance of a very strong band in the region of 881–814 cm<sup>−1</sup> due to the aromatic  $\nu(\text{C}—\text{H})$  out-of plane bending vibrations suggests the presence of *para*-disubstituted benzene rings. In addition to these bands, medium intensity bands appeared in the region of 1664–1443 cm<sup>−1</sup> and 1334–994 cm<sup>−1</sup> are due to aromatic ring  $\nu(\text{C}=\text{C})$  and  $\nu(\text{C}—\text{O})/\nu(\text{C}—\text{N})$  stretching vibrations, respectively.

The <sup>1</sup>H NMR spectrum of bisimines **2–5** (Table 2), showed most characteristic signals in the region of  $\delta$  = 8.51–9.76 ppm due to HC=N functionality along with the corresponding signals due to aryl protons. A significant downfield shifting of HC=N signals are observed as the number of aromatic rings are increased on –HC=N functionality. Whereas the diamines **6–8** showed most characteristic signals as broad singlet in the range of  $\delta$  = 3.75–3.69 ppm due to –NH functionality and a sharp singlet in the range of  $\delta$  = 4.31–5.18 due to –CH<sub>2</sub>Ar benzylic protons respectively. Other signals are observed due to aromatic protons with proper splitting patterns and the assignment of each <sup>1</sup>H signals are well supported by <sup>13</sup>C and DEPT-135 NMR experiments. In the <sup>13</sup>C and DEPT-135 NMR spectra of bisimines **2–4** (Table 2), the characteristic signals appeared in the range of  $\delta$  = 156–160 ppm are attributable to C=N carbon atoms. For diamines **6–7**, signals appeared in the range of  $\delta$  = 40–50 ppm is assigned to benzylic carbon atoms. All other signals observed in the range of  $\delta$  = 110–155 ppm are due to aromatic carbons. Furthermore, to reinforce the assignments of the NMR data and to obtain the detailed view of the structural elucidation, experiments were carried out using 2D NMR spectroscopy such as homonuclear gCOSY and heteronuclear HSQC experiments on some of the relevant compounds.

Interestingly, <sup>1</sup>H and <sup>13</sup>C NMR data along with 2D NMR study of bisimine **3** bearing anthracenyl substituents at the peripheral positions, suggest the presence of two isomeric species in 43:57 ratios. The possibility of the existence of both *E/Z* isomers in **3** was ruled out as it maintains almost the similar ratios (42:58) even on complete reduction to its benzyl form **7**. Probably, in the presence of the bulkier anthracenyl group, the possible C–C bond rotation is hindered and hence compound **3** and **7** could exist in the form of 43:57 and 42:58 conformer mixtures (a and b), respectively.

COSY experiments of **2** and **3** clearly show correlations between the peak at 7.185/7.390 ppm and 6.650/6.840<sup>a</sup>, 6.740/6.980<sup>b</sup> ppm, respectively. HSQC experiment of **2** shows cross peaks at 7.185/119.60 ppm and 7.390/122.48 ppm whereas compound **3** shows cross peaks at 6.650/116.25<sup>a</sup>, 6.740/116.34<sup>b</sup>, 6.840/119.55<sup>a</sup>, 6.980/121.04<sup>b</sup> ppm. These correlations support the assignment of signals corresponding to diphenyl ether moieties in the molecular framework. Moreover, the COSY experiment of **2** and **3**, does not show any correlation for the peak 9.177 and 9.745<sup>a</sup>, 9.695<sup>b</sup> ppm respectively whereas HSQC experiment of **2** and **3** shows cross peaks at 9.177/159.34 ppm and 9.745/159.09<sup>a</sup>, 9.695/158.48<sup>b</sup> ppm respectively. These correlations support the assignment of signals corresponding to –HC=N functionality present in the respective compounds. The



**Scheme 1.** Synthetic protocol for 4,4'-diaminodiphenyl ether derivatives.

**Table 1**  
Micro-, mass- and IR analysis data for compounds **1–7**.

Entry	Molecular formula (MW)	Yield (%)	Mp (°C)	Elemental analysis (%) found (calculated)			Mass data (m/z)	IR data (KBr disk) $\nu_{\max}/\text{cm}^{-1}$
				C	H	N		
<b>1</b>	—	—	—	—	—	—	—	—
<b>2</b>	C <sub>34</sub> H <sub>24</sub> N <sub>2</sub> O (476.57)	>98	133.3	85.76 (85.69)	5.20 (5.08)	5.92 (5.88)	476.24 (4%)	3042, 2830, 1608, 1483, 1334, 1276, 1239, 1194, 1161, 1099, 831, 794, 769.
<b>3</b>	C <sub>42</sub> H <sub>28</sub> N <sub>2</sub> O (576.68)	97	197.0	87.55 (87.47)	4.98 (4.89)	4.95 (4.86)	576.49 (40%), 577.48 (34%), 578.53 (24%)	3042, 2874, 1664, 1617, 1555, 1530, 1488, 1443, 1312, 1242, 1144, 954, 881, 724.
<b>4</b>	C <sub>42</sub> H <sub>28</sub> N <sub>2</sub> O (576.68)	91	—	87.55 (87.47)	4.50 (4.89)	4.94 (4.86)	577.50 (2%)	3042, 2906, 1664, 1617, 1555, 1530, 1488, 1443, 1312, 1242, 1144, 994, 881, 724.
<b>5</b>	—	—	—	—	—	—	—	—
<b>6</b>	C <sub>34</sub> H <sub>28</sub> N <sub>2</sub> O (480.60)	70	—	85.12 (84.97)	5.98 (5.87)	5.99 (5.83)	480.18 (5%)	3373, 3012, 1597, 1513, 1497, 1390, 1309, 1222, 1110, 1063, 864, 825, 802, 772.
<b>7</b>	C <sub>42</sub> H <sub>32</sub> N <sub>2</sub> O (580.72)	55	—	86.98 (86.87)	5.69 (5.55)	4.99 (4.82)	581.71 (2%)	3389, 2958, 1617, 1510, 1494, 1396, 1306, 1261, 1216, 1105, 1094, 1012, 867, 814, 794, 730.

COSY experiment of **6** and **7** do not show any correlation for the peak 4.733 ppm and 5.153<sup>a</sup>, 5.177<sup>b</sup> ppm respectively whereas HSQC experiment shows two distinct cross peaks at 4.733/47.10, 47.12 ppm for **6** and cross peaks at 5.153<sup>a</sup>, 5.177<sup>b</sup>/41.493<sup>(a+b)</sup> ppm respectively which are assigned to the benzylic –CH<sub>2</sub> functionality. Similarly, the assignments of remaining <sup>1</sup>H, <sup>13</sup>C signals are based on DEPT-135, COSY and HSQC 2D NMR experiments. The IR, <sup>1</sup>H, <sup>13</sup>C NMR and 2D NMR correlation experiment data for **2–3** and **6–7** are in good agreement with those observed for the similar types of compounds reported in the literature [14,16]. All compounds synthesized were characterized by mass spectroscopy, the peaks detected corresponding to the molecular ion  $m/z = (M + 1)$  and  $m/z = (M + Na)$  gives the evidence for the formation of the compounds.

## 2.2. UV–visible absorption, emission and optical properties of **1–7**

The UV–visible absorption and emission spectra of **1–7** were measured at room temperature from 10<sup>−4</sup> M CH<sub>2</sub>Cl<sub>2</sub> solution samples and the pertinent results (Table 3) are in accordance with the literature reports on closely related compounds [17]. In the UV–visible absorption spectra of all compounds (Fig. 1), the shorter absorption band (240–300 nm) is assigned to  $\pi \rightarrow \pi^*$  transitions and the longer absorption band (300–415 nm) is assigned to  $n \rightarrow \pi^*$  transitions.

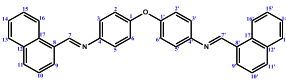
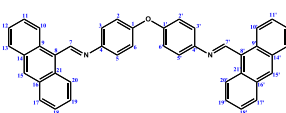
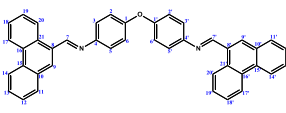
It appears that the  $\lambda_{\max}$  value for compounds **2–7**, arises from  $\pi \rightarrow \pi^*$  transition, are similar ~250 nm and remains unaffected by the polyaromatic substituents present on peripheral positions. However, compound **1** absorbs at  $\lambda_{\max} = 317$  nm due to  $n \rightarrow \pi^*$  transition with the highest value of the molar extinction coefficient (67,944). Bisimines **3** and **4** bearing anthranyl and phenanthrenyl substituents showed absorption bands at higher wavelengths >400 nm due to extended delocalization of  $\pi$  electrons. A considerable blue shifts in the  $n \rightarrow \pi^*$  transition bands have been observed in the bisimine compounds with the increase in the number of rings of polyaromatic substituents, suggesting electron withdrawing tendency of polyaromatic substituents.

On the other hand, a fluorescence quenching effect of imine moiety is clearly seen in the UV–visible emission spectra of bisimines **1–4** (Fig. 2). This is resulted from favorable orbital overlap between imine-nitrogen and the  $p$  orbital of conjugated phenyl rings, causing photoinduced electron transfer [18]. The imine groups as linkers between the phenyl rings make the system rigid and the lone pair of electrons on nitrogen atoms is delocalized onto the  $\pi$ -electron system of the conjugated phenyl rings and thus provides a favorable orbital overlap. The earlier studies suggest that

the fluorescence properties are greatly depends upon the molecular arrangements, achieved by means of polymorphism, conformational rigidity of the fluorophore (dihedral angles), intermolecular interactions  $\pi \cdots \pi$  or C–H $\cdots\pi$  interactions and upon the nature of substituents [17,19]. Obviously, bisimine **1** and **3** bearing benzylidene and 9-anthranylmethylidene substituents shows very weak emission from locally excited ( $n \rightarrow \pi^*$ ) state at room temperature as compared to the corresponding diamine compound **5** and **7** respectively, due to the quenching effect of imine moiety (vide supra). However the emission intensity of bisimine **2** bearing naphthylmethylidene substituents is comparable to the corresponding diamine **6**. The results of emission study suggest that the emission intensities are dependent on not only the possible weak interactions but also on immobilization of the polyaromatic substituents, which suppresses the distortion of the molecular framework and the concomitant nonradiative decay process. Moreover, the absorption and emission spectra of each compounds **1–7** showed similar patterns i.e. two or more kinds of fluorescence emission bands are appearing by the excitation of two or more kinds of absorption bands (in any case, shoulder is appearing). It is to be noted that the emission wavelengths of the conjugated aromatic bisimines **1, 2** are considerably lower (~55 nm) than the emission wavelengths of the conjugated polyaromatic bisimines **3, 4**. Moreover considerable red shifts (a shift range of approximately 65 nm) of the emission wavelengths of bisimines **1** and **3** were observed upon the reduction to corresponding diamines **5** and **7**. Contrarily, a significant blue shift of the emission wavelengths of bisimine **2** of 66 nm was observed on the reduction to corresponding diamine **6**.

Compounds **1–7** were further investigated for their optical behavior towards wide band-gap semiconducting nature using UV–visible transmittance measurements. The values of the optical energy band gap for **1–7** were obtained from the photon absorption corresponding to electronic excitation from the valence band to the conduction band as described elsewhere [13]. The results suggest that the absorption in these samples corresponds to a direct energy gap and the band gap value ( $E_g$ ), obtained by extrapolating the linear part of the Tauc plot (with  $c = 1/2$ ) is summarized in Table 3. All compounds **1–7** exhibits the feature of a direct band gap semiconductor. The values of  $E_g$  for bisimine compounds **1–4**, decrease in the order  $1 > 2 > 3 > 4$  as the number of rings in the polyaromatic substituents increases. However, the band gap energies for diamines **5–7** are considerably lower than bisimines. The lower values of band gap energies for diamines are obvious, as polyamines are widely explored as semiconducting materials.

**Table 2**  
NMR spectral data for **2–4** and **6–7**.

Entry	Structures	NMR data (ppm)				
		<sup>1</sup> H and <sup>13</sup> C		2D NMR correlation expts.		
		<sup>1</sup> H NMR	<sup>13</sup> C NMR	DEPT-135	<sup>1</sup> H– <sup>1</sup> H (COSY)	<sup>1</sup> H– <sup>13</sup> C (HSQC)
<b>1</b>	–	–	–	–	–	–
<b>2</b>		7.185 (d, 4H, <b>3,5,3',5'</b> ; <i>J</i> = 8.4 Hz); 7.390 (d, 4H, <b>2,6,2',6'</b> ; <i>J</i> = 8.4 Hz); 7.619 (m, 4H, <b>11,15,11',15'</b> ; <i>J</i> = 8.4, 8.0, 7.2 Hz); 7.680 (dd, 2H, <b>10,10'</b> ; <i>J</i> = 8.0, 7.2 Hz); 7.964 (d, 2H, <b>13,13'</b> ; <i>J</i> = 8.0 Hz); 8.013 (d, 2H, <b>14,14'</b> ; <i>J</i> = 8.0 Hz); 8.146 (d, 2H, <b>16,16'</b> ; <i>J</i> = 7.2 Hz); 9.110 (d, 2H, <b>9,9'</b> ; <i>J</i> = 8.4 Hz); 9.177 (s, 2H, <b>7,7'</b> ).	119.60 ( <b>3,5,3',5'</b> ), 122.52 ( <b>2,6,2',6'</b> ), 124.33 ( <b>9,9'</b> ), 125.42, 126.32 ( <b>11,15,11',15'</b> ), 127.55 ( <b>10,10'</b> ), 128.88 ( <b>13,13'</b> ), 129.87 ( <b>16,16'</b> ), 131.53 ( <b>12,17,12',17'</b> ), 131.96 ( <b>14,14'</b> ), 133.98 ( <b>8,8'</b> ), 148.02 ( <b>4,4'</b> ), 155.87 ( <b>1,1'</b> ), 159.34 ( <b>7,7'</b> ).	119.57 ( <b>3,5,3',5'</b> ), 122.48 ( <b>2,6,2',6'</b> ), 124.26 ( <b>9,9'</b> ), 125.39, 126.30 ( <b>11,15,11',15'</b> ), 127.52 ( <b>10,10'</b> ), 128.85 ( <b>13,13'</b> ), 129.80 ( <b>16,16'</b> ), 131.95 ( <b>14,14'</b> ), 159.34 ( <b>7,7'</b> ).	7.185 ( <b>3,5,3',5'</b> ) couple with 7.390 ( <b>2,6,2',6'</b> ); 7.619 ( <b>11,15,11',15'</b> ) couple with 7.680 ( <b>10,10'</b> ), 7.964 ( <b>13,13'</b> ), 8.013 ( <b>14,14'</b> ) and 8.146 ( <b>16,16'</b> ); 7.680 ( <b>10,10'</b> ) couple with 9.110 ( <b>9,9'</b> ).	7.185 ( <b>3,5,3',5'</b> ) and 119.57 ( <b>3,5,3',5'</b> ); 7.390 ( <b>2,6,2',6'</b> ) and 122.48 ( <b>2,6,2',6'</b> ); 7.619 ( <b>11,15,11',15'</b> ), 7.680 ( <b>10,10'</b> ) and 127.52 ( <b>10,10'</b> ); 7.964 ( <b>13,13'</b> ) and 128.85 ( <b>13,13'</b> ); 8.013 ( <b>14,14'</b> ) and 131.95 ( <b>14,14'</b> ); 8.146 ( <b>16,16'</b> ) and 129.80 ( <b>16,16'</b> ); 9.110 ( <b>9,9'</b> ) and 124.26 ( <b>9,9'</b> ); 9.177 ( <b>7,7'</b> ) and 159.34 ( <b>7,7'</b> ).
<b>3</b>		6.650 (d, 4H, <b>3,5,3',5'</b> ; <i>J</i> = 6.8 Hz) <sup>a</sup> ; 6.740 (d, 4H, <b>3,5,3',5'</b> ; <i>J</i> = 6.8 Hz) <sup>b</sup> ; 6.840 (d, 4H, <b>2,6,2',6'</b> ; <i>J</i> = 6.8 Hz) <sup>b</sup> ; 6.980 (d, 4H, <b>2,6,2',6'</b> ; <i>J</i> = 6.8 Hz) <sup>b</sup> ; 7.107 (d, 2H, <b>13,13'</b> ; <i>J</i> = 8.8 Hz) <sup>b</sup> ; 7.272 (d, 2H, <b>13,13'</b> ; <i>J</i> = 7.6 Hz) <sup>a</sup> ; 7.440 (d, 2H, <b>12,12'</b> ; <i>J</i> = 6.8 Hz) <sup>b</sup> ; 7.510–7.616 (m, <b>11,17,18,19,11',17',18',19'</b> ) <sup>a+b</sup> ; 8.060 (d, 2H, <b>10,10'</b> ; <i>J</i> = 7.2 Hz) <sup>b</sup> ; 8.079 (d, 2H, <b>10,10'</b> ; <i>J</i> = 7.2 Hz) <sup>b</sup> ; 8.557 (s, 2H, <b>15,15'</b> ); 8.580 (s, 2H, <b>15,15'</b> ) <sup>a</sup> ; 8.737 (d, 2H, <b>20,20'</b> ; <i>J</i> = 8.8 Hz) <sup>a</sup> ; 8.782 (d, 2H, <b>20,20'</b> ; <i>J</i> = 8.8 Hz) <sup>a</sup> ; 9.695 (s, 2H, <b>7,7'</b> ) <sup>a</sup> ; 9.745 (s, 2H, <b>7,7'</b> ) <sup>a</sup> .	116.25 ( <b>3,5,3',5'</b> ) <sup>a</sup> ; 116.34 ( <b>3,5,3',5'</b> ) <sup>b</sup> ; 118.07 ( <b>13,13'</b> ) <sup>b</sup> ; 119.55 ( <b>2,6,2',6'</b> ) <sup>a</sup> ; 119.69 ( <b>13,13'</b> ) <sup>a</sup> ; 121.04 ( <b>2,6,2',6'</b> ) <sup>b</sup> ; 122.38 ( <b>12,12'</b> ) <sup>b</sup> ; 122.61 ( <b>12,12'</b> ) <sup>a</sup> ; 124.77 ( <b>20,20'</b> ) <sup>a</sup> ; 124.82 ( <b>20,20'</b> ) <sup>b</sup> ; 125.43, 125.47, 127.22, 127.33 ( <b>11,17,18,19,11',17',18',19'</b> ) <sup>a+b</sup> ; 127.53 ( <b>14,14'</b> ) <sup>a</sup> ; 129.06 ( <b>10,10'</b> ) <sup>b</sup> ; 129.11 ( <b>10,10'</b> ) <sup>a</sup> ; 130.50 ( <b>15,15'</b> ) <sup>b</sup> ; 130.59, 130.65 ( <b>14,16,14',16'</b> ) <sup>b</sup> ; 130.72 ( <b>15,15'</b> ) <sup>a</sup> ; 131.35 ( <b>16,16'</b> ) <sup>a</sup> ; 141.70 ( <b>9,21,9',21'</b> ) <sup>a</sup> ; 142.81 ( <b>9,21,9',21'</b> ) <sup>b</sup> ; 146.88 ( <b>8,8'</b> ) <sup>b</sup> ; 148.02 ( <b>8,8'</b> ) <sup>a</sup> ; 148.80 ( <b>4,4'</b> ) <sup>b</sup> ; 150.62 ( <b>4,4'</b> ) <sup>a</sup> ; 156.11 ( <b>1,1'</b> ) <sup>a</sup> ; 157.75 ( <b>1,1'</b> ) <sup>b</sup> ; 158.48 ( <b>7,7'</b> ) <sup>b</sup> ; 159.09 ( <b>7,7'</b> ) <sup>a</sup> .	116.24 ( <b>3,5,3',5'</b> ) <sup>a</sup> ; 116.33 ( <b>3,5,3',5'</b> ) <sup>b</sup> ; 118.06 ( <b>13,13'</b> ) <sup>b</sup> ; 119.54 ( <b>2,6,2',6'</b> ) <sup>a</sup> ; 119.68 ( <b>13,13'</b> ) <sup>a</sup> ; 121.04 ( <b>2,6,2',6'</b> ) <sup>b</sup> ; 122.37 ( <b>12,12'</b> ) <sup>b</sup> ; 122.60 ( <b>12,12'</b> ) <sup>a</sup> ; 124.77 ( <b>20,20'</b> ) <sup>a</sup> ; 124.81 ( <b>20,20'</b> ) <sup>b</sup> ; 125.42, 125.47, 127.22, 127.33 ( <b>11,17,18,19,11',17',18',19'</b> ) <sup>a+b</sup> ; 129.06 ( <b>10,10'</b> ) <sup>b</sup> ; 129.11 ( <b>10,10'</b> ) <sup>a</sup> ; 130.49 ( <b>15,15'</b> ) <sup>b</sup> ; 130.72 ( <b>15,15'</b> ) <sup>a</sup> ; 158.48 ( <b>7,7'</b> ) <sup>b</sup> ; 159.09 ( <b>7,7'</b> ) <sup>a</sup> .	6.650 ( <b>3,5,3',5'</b> ) <sup>a</sup> couple with 6.840 ( <b>2,6,2',6'</b> ) <sup>a</sup> ; 6.740 ( <b>3,5,3',5'</b> ) <sup>b</sup> couple with 6.980 ( <b>2,6,2',6'</b> ) <sup>b</sup> ; 7.107 ( <b>13,13'</b> ) <sup>b</sup> couple with 7.440 ( <b>12,12'</b> ) <sup>b</sup> ; 7.510–7.616 ( <b>11,17,18,19,11',17',18',19'</b> ) <sup>a+b</sup> couple with 7.272 ( <b>13,13'</b> ) <sup>a</sup> ; 8.060 ( <b>10,10'</b> ) <sup>b</sup> , 8.079 ( <b>10,10'</b> ) <sup>a</sup> , 8.737 ( <b>20,20'</b> ) <sup>b</sup> and 8.782 ( <b>20,20'</b> ) <sup>a</sup> .	6.650 ( <b>3,5,3',5'</b> ) <sup>a</sup> and 116.25 ( <b>3,5,3',5'</b> ) <sup>b</sup> ; 6.740 ( <b>3,5,3',5'</b> ) <sup>b</sup> and 116.34 ( <b>3,5,3',5'</b> ) <sup>a</sup> ; 6.840 ( <b>2,6,2',6'</b> ) <sup>a</sup> and 119.55 ( <b>2,6,2',6'</b> ) <sup>b</sup> ; 6.980 ( <b>2,6,2',6'</b> ) <sup>b</sup> and 121.04 ( <b>2,6,2',6'</b> ) <sup>a</sup> ; 7.107 ( <b>13,13'</b> ) <sup>b</sup> and 118.07 ( <b>13,13'</b> ) <sup>a</sup> ; 7.272 ( <b>13,13'</b> ) <sup>a</sup> and 119.69 ( <b>13,13'</b> ) <sup>b</sup> ; 7.440 ( <b>12,12'</b> ) <sup>b</sup> and 122.38 ( <b>12,12'</b> ) <sup>a</sup> ; 7.510–7.616 ( <b>11,17,18,19,11',17',18',19'</b> ) <sup>a+b</sup> and 125.43, 125.47, 127.22, 127.33 ( <b>11,17,18,19,11',17',18',19'</b> ) <sup>a+b</sup> ; 8.060 ( <b>10,10'</b> ) <sup>b</sup> and 129.06 ( <b>10,10'</b> ) <sup>a</sup> ; 8.079 ( <b>10,10'</b> ) <sup>a</sup> and 129.11 ( <b>10,10'</b> ) <sup>b</sup> ; 8.557 ( <b>15,15'</b> ) <sup>b</sup> and 130.49 ( <b>15,15'</b> ) <sup>a</sup> ; 8.580 ( <b>15,15'</b> ) <sup>a</sup> and 130.72 ( <b>15,15'</b> ) <sup>b</sup> ; 8.737 ( <b>20,20'</b> ) <sup>b</sup> and 124.82 ( <b>20,20'</b> ) <sup>a</sup> ; 8.782 ( <b>20,20'</b> ) <sup>a</sup> and 124.77 ( <b>20,20'</b> ) <sup>b</sup> ; 9.695 ( <b>7,7'</b> ) <sup>b</sup> and 158.48 ( <b>7,7'</b> ) <sup>a</sup> ; 9.745 ( <b>7,7'</b> ) <sup>a</sup> and 159.09 ( <b>7,7'</b> ) <sup>b</sup> .
<b>4</b>		7.260 (d, 4H, <b>3,5,3',5'</b> ; <i>J</i> = 5.6 Hz); 7.51 (d, 4H, <b>2,6,2',6'</b> ; <i>J</i> = 5.6 Hz); 7.574 (m, 4H, Ph); 7.835 (m, 2H, Ph) 8.085 (d, 4H, <b>11,11',20',20'</b> ; <i>J</i> = 4.8 Hz); 8.345 (d, 4H, Ph); <i>J</i> = 5.6 Hz); 8.604 (s, 2H, <b>9,9'</b> ); 8.785 (d, 2H, Ph); <i>J</i> = 8.8 Hz); 9.753 (s, 2H, <b>7,7'</b> ).	119.68, 121.94, 122.61, 122.66, 123.56, 124.75, 125.46, 125.73, 126.58, 126.93, 127.24, 127.33, 127.64, 128.58, 129.10, 129.19, 129.33, 129.62, 130.28, 130.64, 130.73, 131.09, 131.34, 132.03, 132.66, 133.49, 134.15, 135.35, 137.15, 144.78, 147.90 (Ph), 156.13 ( <b>1,1'</b> ), 159.16 ( <b>7,7'</b> ).	–	–	–

(continued on next page)

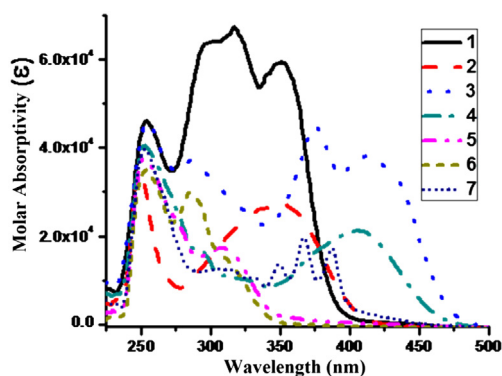
Table 2 (continued)

Entry	Structures	NMR data (ppm)			2D NMR correlation expts.	
		<sup>1</sup> H and <sup>13</sup> C				
		<sup>1</sup> H NMR	<sup>13</sup> C NMR	DEPT-135	<sup>1</sup> H– <sup>13</sup> C (COSY)	<sup>1</sup> H– <sup>13</sup> C (HSQC)
5	–	–	–	–	–	–
6		3.750 (broad s, 2H, <b>NH</b> ); 4.733 (s, 4H, <b>7,7'</b> ); 6.676 (d, 4H, <b>3,5,3',5'</b> ; <i>J</i> = 8.8 Hz); 6.924 (d, 4H, <b>2,6,2',6'</b> ; <i>J</i> = 8.8 Hz); 7.476 (m, 2H, <b>10,10'</b> ) ( <i>J</i> = 7.2 Hz); 7.565 (m, 6H, <b>11,14,15,11',14',15'</b> ; <i>J</i> = 7.2, 2.4 Hz); 7.855 (d, 2H, <b>9,9'</b> ) ( <i>J</i> = 7.64 Hz); 7.935 (d, 2H, <b>13,13'</b> ; <i>J</i> = 8.8 Hz); 8.120 (d, 2H, <b>16,16'</b> ; <i>J</i> = 7.2 Hz).	47.12 ( <b>7,7'</b> ), 113.74 ( <b>3,5,3',5'</b> ), 119.66 ( <b>2,6,2',6'</b> ), 123.68 ( <b>16,16'</b> ), 125.61 ( <b>10,10'</b> ), 125.90, 126.14 and 126.39 ( <b>11,14,15,11',14',15'</b> ), 128.23 ( <b>9,9'</b> ), 128.82 ( <b>13,13'</b> ), 131.58 ( <b>12,12'</b> ), 133.89 ( <b>17,17'</b> ), 134.46 ( <b>8,8'</b> ), 144.07 ( <b>4,4'</b> ), 150.05 ( <b>1,1'</b> ).	47.10 and 47.12 ( <b>7,7'</b> ), 113.74 and 113.75 ( <b>3,5,3',5'</b> ), 119.70 ( <b>2,6,2',6'</b> ), 123.71 ( <b>16,16'</b> ), 125.64 ( <b>10,10'</b> ), 125.94, 126.15 and 126.42 ( <b>11,14,15,11',14',15'</b> ), 128.25 ( <b>9,9'</b> ), 128.85 ( <b>13,13'</b> ).	6.67 ( <b>3,5,3',5'</b> ) couple with 6.924 ( <b>2,6,2',6'</b> ); 7.476 ( <b>10,10'</b> ) couple with 7.855 ( <b>9,9'</b> ) and 7.566 ( <b>11,14,15,11',14',15'</b> ); 7.566 ( <b>11,14,15,11',14',15'</b> ) couple with 7.576 ( <b>10,10'</b> ), 7.935 ( <b>13,13'</b> ) and 8.120 ( <b>16,16'</b> ).	4.733 ( <b>7,7'</b> ) and 47.10, 47.12 ( <b>7,7'</b> ); 6.676 ( <b>3,5,3',5'</b> ) and 113.74, 113.75; 6.924 ( <b>2,6,2',6'</b> ) and, 119.70 ( <b>2,6,2',6'</b> ); 7.476 ( <b>10,10'</b> ) and 125.64 ( <b>10,10'</b> ); 7.566 ( <b>11,14,15,11',14',15'</b> ) and 125.94, 126.15, 126.42 ( <b>11,14,15,11',14',15'</b> ); 7.855 ( <b>9,9'</b> ) and 128.25 ( <b>9,9'</b> ); 7.935 ( <b>13,13'</b> ) and 128.85 ( <b>13,13'</b> ); 8.120 ( <b>16,16'</b> ) and 123.71 ( <b>16,16'</b> ).
7		3.688 (bs, 2H, <b>NH</b> ); 5.153 (s, 2H, <b>7,7'</b> ); 5.177 (s, 2H, <b>7,7'</b> ); 6.653 (d, 4H, <b>3,5,3',5'</b> ); 6.670 (d, 2H, <b>3,3'</b> ; <i>J</i> = 8.8 Hz); 6.800 (d, 2H, <b>5,5'</b> ; <i>J</i> = 8.8 Hz); 6.820 (d, 4H, <b>2,6,2',6'</b> ; <i>J</i> = 8.8 Hz); 6.890 (d, 2H, <b>2,2'</b> ; <i>J</i> = 8.8 Hz); 6.985 (d, 2H, <b>6,6'</b> ; <i>J</i> = 8.8 Hz); 7.030 (d, 2H, <b>13,13'</b> ; <i>J</i> = 8.8 Hz); 7.050 (d, 2H, <b>13,13'</b> ; <i>J</i> = 8.8 Hz); 7.515 (m, 10H, <b>11,12,17,18,19,11',12,17',18',19'</b> ; <i>J</i> = 8.8, 1.9 Hz); 8.060 (d, 2H, <b>10,10'</b> ; <i>J</i> = 8.8 Hz); 8.078 (d, 2H, <b>10,10'</b> ; <i>J</i> = 8.8 Hz); 8.315 (d, 2H, <b>20,20'</b> ; <i>J</i> = 8.8 Hz); 8.335 (d, 2H, <b>20,20'</b> ; <i>J</i> = 8.8 Hz); 8.510 (s, 2H, <b>15,15'</b> ); <i>J</i> = 8.8 Hz).	41.53 ( <b>7,7'</b> ), 113.58 ( <b>5,5'</b> ), 113.68 ( <b>2,6,2',6'</b> ), 116.24 ( <b>3,5,3',5'</b> ), 116.29 ( <b>3,3'</b> ), 119.46 ( <b>2,6,2',6'</b> ), 119.55 ( <b>2,6,2',6'</b> ), 119.76 ( <b>13,13'</b> ), 119.85 ( <b>13,13'</b> ), 124.21 ( <b>20,20'</b> ), 125.19 and 126.50 ( <b>11,12,17,18,19,11',12,17',18',19'</b> ), 127.95 ( <b>15,15'</b> ), 129.15 ( <b>10,10'</b> ), 130.45 ( <b>9,21,9',21'</b> ), 131.52 ( <b>9,21,9',21'</b> ), 141.63 ( <b>14,16,14',16'</b> ), 141.69 ( <b>14,16,14',16'</b> ), 144.40 ( <b>4,4'</b> ), 149.93, 150.20 ( <b>1,1'</b> ), 150.61, 150.88 ( <b>1,1'</b> ).	41.493 ( <b>7,7'</b> ), 113.58 ( <b>5,5'</b> ), 113.62 ( <b>2,6,2',6'</b> ), 116.24 ( <b>3,5,3',5'</b> ), 116.29 ( <b>3,3'</b> ), 119.46 ( <b>2,6,2',6'</b> ), 119.55 ( <b>2,6,2',6'</b> ), 119.76 ( <b>13,13'</b> ), 119.85 ( <b>13,13'</b> ), 124.21 ( <b>20,20'</b> ), 125.19 and 126.50 ( <b>11,12,17,18,19,11',12,17',18',19'</b> ), 127.95 ( <b>15,15'</b> ), 129.15 ( <b>10,10'</b> ).	6.653 ( <b>3,5,3',5'</b> ) couple with 6.820 ( <b>2,6,2',6'</b> ); 6.670 ( <b>3,3'</b> ) couple with 6.890 ( <b>2,2'</b> ); 6.800 ( <b>5,5'</b> ) couple with 6.985 ( <b>6,6'</b> ); 7.515 ( <b>11,12,17,18,19,11',12,17',18',19'</b> ) couple with 7.030 ( <b>13,13'</b> ); 7.050 ( <b>13,13'</b> ), 8.060 ( <b>10,10'</b> ); 8.078 ( <b>10,10'</b> ); 8.315 ( <b>20,20'</b> ) and 8.335 ( <b>20,20'</b> ).	5.153 ( <b>7,7'</b> ), 5.177 ( <b>7,7'</b> ) and 41.493 ( <b>7,7'</b> ); 6.653 ( <b>3,5,3',5'</b> ) and 116.24 ( <b>3,5,3',5'</b> ); 6.670 ( <b>3,3'</b> ) and 116.29 ( <b>3,3'</b> ); 6.800 ( <b>5,5'</b> ) and 113.58 ( <b>5,5'</b> ); 6.820 ( <b>2,6,2',6'</b> ) and 113.62, 119.55 ( <b>2,6,2',6'</b> ); 6.890 ( <b>2,2'</b> ); 6.985 ( <b>6,6'</b> ) and 119.46 ( <b>2,6,2',6'</b> ); 7.030 ( <b>13,13'</b> ) and 119.76 ( <b>13,13'</b> ); 7.050 ( <b>13,13'</b> ) and 119.85 ( <b>13,13'</b> ); 7.515 ( <b>11,12,17,18,19,11',12,17',18',19'</b> ) and 125.19 and 126.50 ( <b>11,12,17,18,19,11',12,17',18',19'</b> ); 8.060 ( <b>10,10'</b> ); 8.078 ( <b>10,10'</b> ) and 129.15 ( <b>10,10'</b> ); 8.315 ( <b>20,20'</b> ); 8.335 ( <b>20,20'</b> ) and 124.21 ( <b>20,20'</b> ); 8.510 (s, 2H, <b>15,15'</b> ) and 127.95 ( <b>15,15'</b> ).



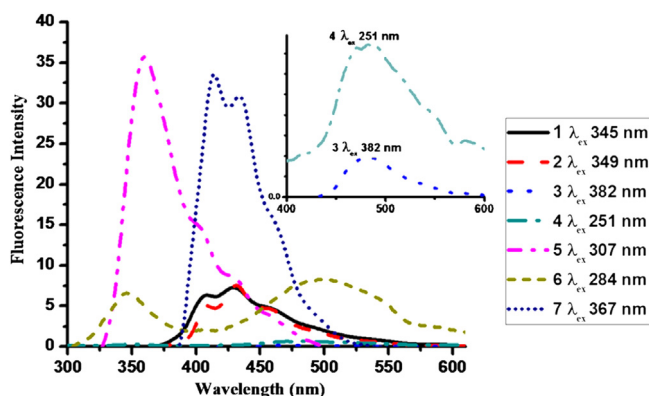
**Table 3**UV–visible absorption, emission and optical band gap data for **1–7**.

Entry	UV–visible spectral data ( $10^{-4}$ M CH <sub>2</sub> Cl <sub>2</sub> ) $\lambda_{\max}$ nm ( $\epsilon$ , L mol <sup>-1</sup> cm <sup>-1</sup> )	Emission spectral data ( $10^{-4}$ M CH <sub>2</sub> Cl <sub>2</sub> )		Band gap $E_g$ (eV)
		$\lambda_{\text{em}}$ nm (intensity)	$\lambda_{\text{ex}}$ (nm)	
<b>1</b>	253 (47,052) $\pi \rightarrow \pi^*$ (phenyl)	407 (6.3185) $\pi^* \rightarrow n$ (imine)	345	3.0316
	297 (60,420) $\pi \rightarrow \pi^*$ (imine)	428 (7.2773) $\pi^* \rightarrow n$ (imine)		
	317 (67,944) $n \rightarrow \pi^*$ (imine)			
	345 (67,458) $n \rightarrow \pi^*$ (imine)			
<b>2</b>	249 (34,554) $\pi \rightarrow \pi^*$ (phenyl)	408 (5.0008) $\pi^* \rightarrow n$ (imine)	349	2.8554
	350 (27,193) $n \rightarrow \pi^*$ (imine)	431 (7.5310) $\pi^* \rightarrow n$ (imine)		
		456 (4.7134) $\pi^* \rightarrow n$ (imine)		
		474 (0.1616) $\pi^* \rightarrow n$ (imine)		
<b>3</b>	254 (45,826) $\pi \rightarrow \pi^*$ (phenyl)	485 (0.1692) $\pi^* \rightarrow n$ (imine)	382	2.5067
	286 (37,195) $\pi \rightarrow \pi^*$ (imine)			
	375 (44,997) $n \rightarrow \pi^*$ (imine)			
	411 (38,025) $n \rightarrow \pi^*$ (imine)			
<b>4</b>	252 (40,461) $\pi \rightarrow \pi^*$ (phenyl)	481 (0.6584) $\pi^* \rightarrow \pi$ (phenyl)	251	2.4072
	291 (17,193) $\pi \rightarrow \pi^*$ (imine)	491 (0.6488) $\pi^* \rightarrow \pi$ (phenyl)		
	406 (21,256) $n \rightarrow \pi^*$ (imine)			
<b>5</b>	253 (38,616) $\pi \rightarrow \pi^*$ (phenyl)	360 (35.6569) $\pi^* \rightarrow n$ (amine)	307	2.1677
	277 (23,066) $\pi \rightarrow \pi^*$ (amine)			
	307 (17,366) $n \rightarrow \pi^*$ (amine)			
<b>6</b>	253 (35,066) $\pi \rightarrow \pi^*$ (phenyl)	346 (6.5753) $\pi^* \rightarrow \pi$ (amine)	284	2.2897
	285 (29,934) $\pi \rightarrow \pi^*$ (amine)	497 (8.2707) $\pi^* \rightarrow \pi$ (amine)		
	313 (14,241) $n \rightarrow \pi^*$ (amine)			
<b>7</b>	253 (39,699) $\pi \rightarrow \pi^*$ (phenyl)	414 (33.5127) $\pi^* \rightarrow n$ (amine)	367	2.3853
	349 (13,627) $n \rightarrow \pi^*$ (amine)	434 (31.0034) $\pi^* \rightarrow n$ (amine)		
	367 (19,653) $n \rightarrow \pi^*$ (amine)			
	387 (17,280) $n \rightarrow \pi^*$ (amine)			

**Fig. 1.** UV–visible absorption spectra of compounds **1–7** in  $10^{-4}$  M CH<sub>2</sub>Cl<sub>2</sub> solution.

### 2.3. Thermogravimetric studies for **1–7**

A thermogravimetric study of **1–7**, performed at a heating rate of 10 °C/min under N<sub>2</sub> atmosphere from room temperature to 550 °C and thermal analysis data for **1–7** is summarized in Table 4. The peaks on DTG and corresponding DTA curves confirm a single or multi stage

**Fig. 2.** UV–visible emission spectra of compounds **1–7** in  $10^{-4}$  M CH<sub>2</sub>Cl<sub>2</sub> solution.

mass loss for these compounds. The DTA curves exhibits first endothermic peak without any significant mass loss on DTG curves for each compound, due to the phase change that can be assigned to the melting points of the respective compounds (except compound **6** and **7**). Other peaks of DTA curves are attributed to endothermic and/or exothermic elimination of molecular fragments due to the thermal degradation, confirmed by peaks on DTG curves. Being organic, all the compounds, except **3** shows >71% mass loss up to the temperature 550 °C. The extra thermal stability of compound **3** may be caused by the presence of extended conjugation and intermolecular  $\pi \cdots \pi$  or C–H $\cdots\pi$  interactions possibly taking place in the solid state. Compound **1** showed ~99% mass loss up to 410 °C, which can be attributed to either almost complete thermal degradation or evaporation

**Table 4**Thermogravimetric data for **1–7**.

Entry	Mp °C	Mass loss% (temperature range °C)	Residual content	DTG (°C)	DTA (°C)
1	185.4	99.6% (300–410)	—	410	285.4 (–6.36 uV), 400.8 (–6.43 uV)
2	133.3	71.2% (100–500)	Mass loss continues after 550 °C	454.5	122.2 (5.51 uV), 133.3 (3.13 uV), 457.8 (–2.02 uV), 197.0 (3.85 uV)
3	197.0	64.9% (100–550)	Mass loss continues after 550 °C	410.7	146.4 (4.57 uV)
4	146.4	34.4% (50–275) 37.0% (275–550)	Mass loss continues after 550 °C	211.1, 402.0	—
5	90.0	93.0% (200–410)	7% char	380.6	90.0 (1.43 uV), 184.3 (–7.97 uV)
6	—	87.3% (100–500)	12.7 char	380.5	—
7	—	87.4% (125–550)	12.6 char	300.1, 350.3, 525.0	—



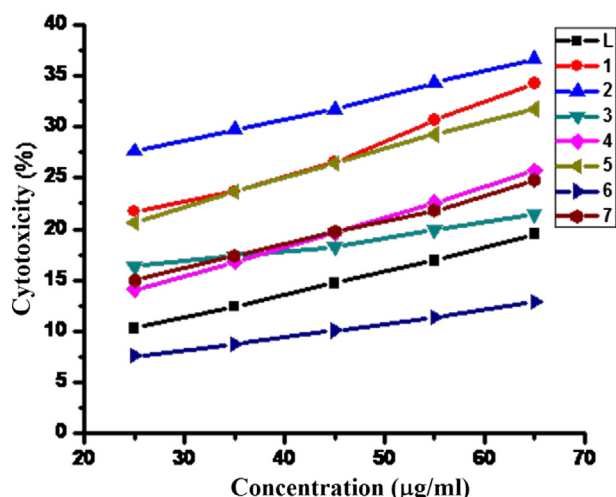


Fig. 3. Concentration versus % inhibition for Hep 3B.

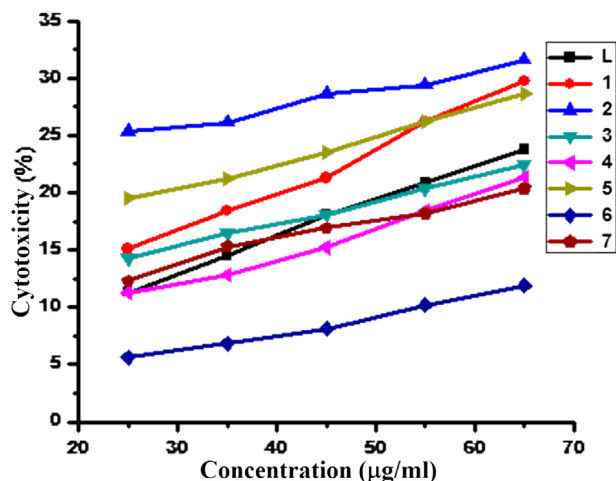
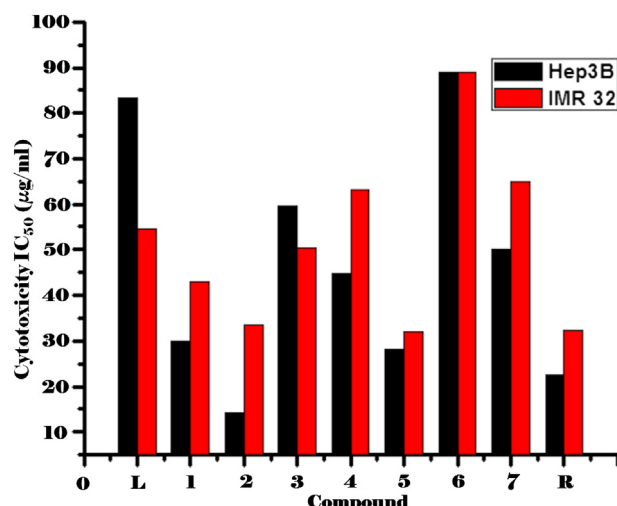


Fig. 4. Concentration versus % inhibition for IMR 32.

of compound at high temperature. Except, compound 4 showing two stages of thermal degradation, all other compounds showed single stage degradation and each of them give a stable residual mass as revealed by their corresponding DTG curves.

**Table 5**  
Cytotoxicity  $IC_{50}$  values for compound 1–7 against Hep 3B and IMR 32 cancer cells.

Entry	Chemical structure	Cytotoxicity $IC_{50}$ ( $\mu\text{g/mL}$ ) $\pm$ SE	
		Hep 3B	IMR 32
L	4,4'-Diaminodiphenyl ether	83.18 $\pm$ 0.43	54.55 $\pm$ 0.48
1	4,4'-Bis(benzylideneamino) diphenyl ether	29.84 $\pm$ 0.86	42.95 $\pm$ 0.59
2	4,4'-Bis(1-naphthyl methylideneamino) diphenyl ether	14.13 $\pm$ 0.39	33.5 $\pm$ 0.23
3	4,4'-Bis(9-anthracenyl methylideneamino) diphenyl ether	59.57 $\pm$ 1.99	50.35 $\pm$ 0.68
4	4,4'-Bis(9-phenanthrenyl methylideneamino) diphenyl ether	44.67 $\pm$ 0.84	63.1 $\pm$ 1.14
5	4,4'-Bis(benzylamino)diphenyl ether	28.18 $\pm$ 1.38	31.92 $\pm$ 0.91
6	4,4'-Bis(1-naphthylmethylamino) diphenyl ether	89.13 $\pm$ 2.11	89.13 $\pm$ 0.93
7	4,4'-Bis(9-anthracenylmethylamino) diphenyl ether	50.12 $\pm$ 1.58	65.01 $\pm$ 0.55
R	Cisplatin	22.39 $\pm$ 0.38	32.36 $\pm$ 0.09


Fig. 5. Cytotoxicity  $IC_{50}$  ( $\mu\text{g/mL}$ ) values for compound 1–7.

#### 2.4. In-vitro cytotoxic activity

Compounds 1–7 and lead compound L was evaluated for their cytotoxic activity by the MTT assay [20] against two malignant tumor cell lines: Hep 3B and IMR 32 and the cytotoxicity were compared with clinically used antineoplastic drug cisplatin (Figs. 3 and 4). The 50% inhibition concentration ( $IC_{50}$ ) values obtained after incubation of 6 h for all the compounds against both the cell lines are summarized in Table 5.

The analysis of the  $IC_{50}$  values suggests that activity of all the compounds enhanced significantly against both malignant tumor cell lines Hep 3B and IMR 32 after derivatization, except 6 which shows lower activity and is not satisfactory as antitumourigenic compound (Fig. 5). Interestingly bisimine 2 and diamine 5 were found extremely active against both Hep 3B ( $IC_{50} = 14.13 \pm 0.39$ ) and IMR 32 ( $IC_{50} = 31.92 \pm 0.91$ ) cell lines respectively and the data suggests that these compounds proved to be more potent as cytotoxic agents than the clinically used antineoplastic drug cisplatin whose  $IC_{50}$  values for Hep 3B and IMR 32 are  $22.39 \pm 0.38$  and  $32.36 \pm 0.09$  respectively. Thus compound 2 is able to significantly arrest the cell proliferation in Hep 3B cell line however its antiproliferative activity ( $IC_{50} = 33.5 \pm 0.23$ ) against IMR 32 cell line is found to be comparable with standard cisplatin

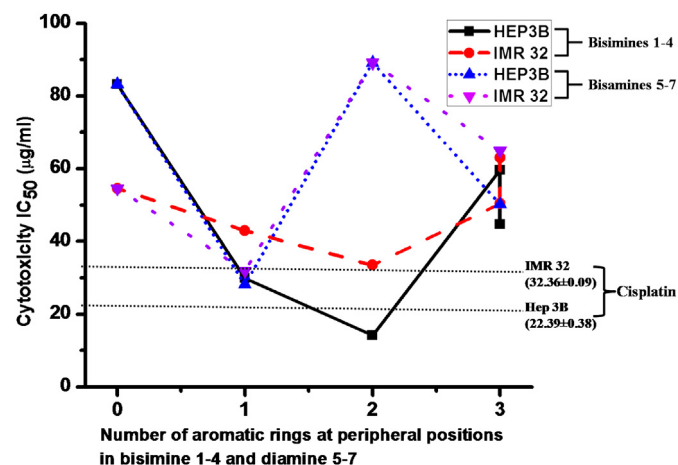
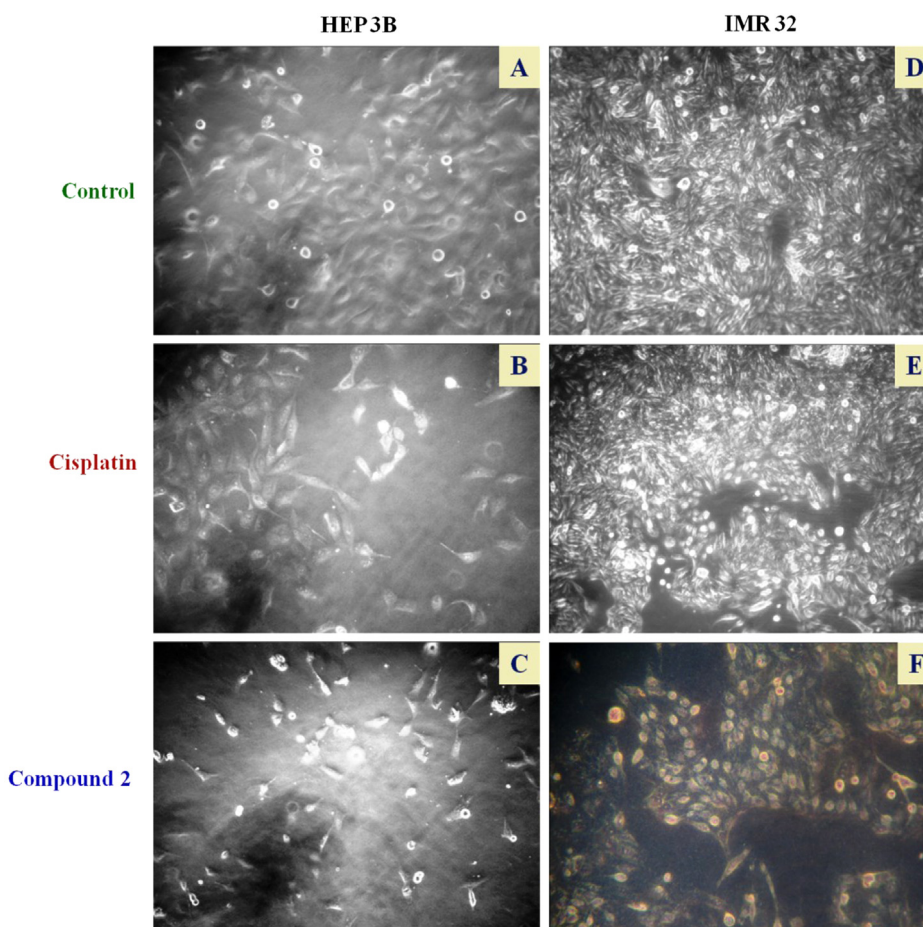


Fig. 6. Impact of the change in the size of polyaromatic hydrocarbon substituents of bisimines and diamine derivatives of L on cytotoxicity.



**Fig. 7.** Microscopic photographs of Hep 3B and IMR 32 cells exposed to the cisplatin (middle row) and the compound **2** (lower row) compared to control (top row) indicating the *in-vitro* anticancer activity. These compounds were assayed at their respective *in-vitro* growth inhibitory  $IC_{50}$  value, as determined using the MTT assay in Hep 3B and IMR 32 cells.

( $IC_{50} = 32.36 \pm 0.09$ ). In general all compounds present better activities against HEP 3B as compared to the activities against IMR 32, except **3** which show better activity against IMR 32. One of the reasons for the enhanced cytotoxic activity of **1–5** and **7** compared to the lead compound **L** could be the increased lipophilicity and

extended  $\pi$ -conjugation of these compounds bearing polyaromatic substituents at peripheral positions, which probably facilitate the stacking interaction of these compounds with the biological targets [21]. We have made an effort to establish a correlation between the observed cytotoxicity of these compounds with the gradual increase in the ring of polyaromatic substituents present on peripheral positions. It appears that the  $IC_{50}$  of bisimine compounds gradually decreases and thus cytotoxicity increases against both the cell lines, as the number of aromatic rings in arylmethylidene substituents increases up to 2 (compound **1** and **2**), however a further increase in aromatic fused rings could not preserve the cytotoxic activity, instead it decreases remarkably (compound **3** and **4**). The presence of bulkier substituents might create barriers for permeability through the cellular membrane; hence less availability of the compound at the site of action could be one of the reasons for the decrease in the cytotoxic activity of **3** and **4**. Similar trends could not be observed in case of diamines **5–7** (Fig. 6).

Since compound **2** had a remarkable activity against both tested human cancer cell lines and the best activity against Hep 3B cell line, it was chosen to be further investigated regarding its mechanism of action. Thus morphological investigations were carried out by using microscopic photographs of both the cell lines Hep 3B and IMR 32 upon 6 h exposure to the compound **2** and standard cisplatin at their respective *in-vitro* growth inhibitory  $IC_{50}$  concentrations. The microscopic photographs are shown in Fig. 7, where A and D show normal proliferation of cells without any insult, B and E show effect of cisplatin on cell growth whereas C and F show less proliferation of cells due to the exposure of compound **2**. The study clearly showed

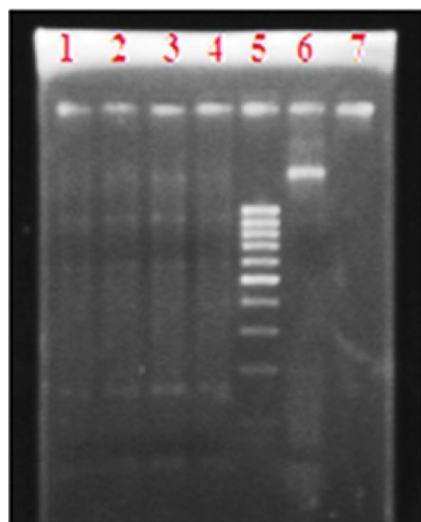


**Fig. 8.** DNA fragmentation assay for compound **2**, **5** and cisplatin. (lane 1, 2: compound **5**; lane 3, 4: compound **2**; lane 5: marker; lane 6, 7: control (cisplatin) at the concentration of their respective  $IC_{50}$  values).

the shrinking of cells, a characteristic apoptotic sign [2], indicating the induction of apoptosis as part of the mechanism of action of these compounds. Further to acquire precision about the mode of action of these compounds, we carried out DNA ladder assay [22] (Fig. 8) to visualize intra-nucleosomal DNA fragmentation (laddering). DNA fragmentation in the form of a ladder due to endonucleolytic attack is reportedly considered as one of the later steps in the apoptotic process or smearing of DNA due to necrosis. Further studies of cytotoxicity and mechanisms of action are underway.

### 3. Conclusion

With our intention to study the impact of different polyaromatic hydrocarbon substituents and bisimine/diamine pharmacophores on cytotoxicity, we have derivatized 4,4'-diaminodiphenyl ether to obtain a novel series of 4,4'-bis(arylmethylideneamino)diphenyl ethers **1–4** and 4,4'-bis(arylmethylamino)diphenyl ethers **5–7**. All the compounds are well characterized by microanalysis, standard spectroscopic methods and by TGA/DTA analysis. The lead compound 4,4'-diaminodiphenyl ether and its derivatives were screened for *in-vitro* antitumor activity against two malignant human cell lines such as Hep 3B and IMR 32 by the MTT assay. Interestingly, some of the derivatives viz **2** and **5** were found remarkably active against both the cell lines and these compounds appeared to be more potent as cytotoxic agents than cisplatin. The DNA fragmentation and microscopic photographs support the induction of apoptosis and explain the mode of action of these derivatives as antitumor agents. The results of emission spectral study of **1–7** suggest that the emission intensities are greatly dependent on immobilization of the polyaromatic substituents which suppresses the distortion of the molecular framework and the concomitant nonradiative decay process. Further the calculated optical band gaps ( $E_g$ ) for **1–7** fall in the range of 2.16–3.03 eV, demonstrating a direct band gap semiconducting nature of these compounds. The extra thermal stability of **3**, may be caused by the presence of extended conjugation and possible intermolecular interactions taking place in the solid state.

### 4. Experimental section

#### 4.1. Material and physical measurements

All the chemicals and solvents used in this work were of laboratory grade available at various commercial sources and used without further purification. The reagents such as 4,4'-diaminodiphenyl ether (99%), sodium borohydride (95%) and 1-naphthaldehyde (95%) were purchased from National Chemicals, Merck and Chemlabs, respectively. 9-formyl anthracene and 9-formyl phenanthrene were synthesized as per the literature procedure [23]. All the reactions and manipulations were performed under an inert atmosphere. Elemental analyses (C, H, N) were performed on a Perkin–Elmer 2400 analyzer. Mass spectra were obtained on Water's QTOF and Thermo Scientific DSQ-II. FT-IR (KBr pellets) spectra were recorded in the 4000–400  $\text{cm}^{-1}$  range using a Perkin–Elmer FT-IR spectrometer. The NMR spectra were obtained on a Bruker AV-III 400 MHz spectrometer in  $\text{CDCl}_3$  unless otherwise noted. The assignments of NMR signals were supported by gCOSY and DEPT-135 and HSQC experiments for the relevant compounds. UV–visible spectra were recorded on a Perkin Elmer Lambda 35 UV–visible spectrophotometer and the optical characterization of solid samples was performed by using the UV–visible transmittance measurements. Fluorescence was recorded on JASCO make spectrofluorometer model FP-6300. TGA/DTA plots were obtained using SII TG/DTA 6300 in flowing  $\text{N}_2$  with a heating rate of 10  $^\circ\text{C min}^{-1}$ .

#### 4.2. Synthesis of **1–7**

##### 4.2.1. General methods for the synthesis of bisimines **2–4**

In a typical procedure, 3 mmol of corresponding aldehydes (468.54 mg of 1-naphthaldehyde **2**, 618.72 mg 9-formyl anthracene **3** or 618.72 mg 9-formyl phenanthrene **4**), a catalytic amount of glacial acetic acid and 1 mmol of 4,4'-diaminodiphenyl ether (200 mg) were added to a freshly distilled toluene (10 mL) and the reaction mixture was allowed to reflux for 2 h using Dean–Stark apparatus. The reaction mixture was cooled at room temperature and solvent was evaporated under vacuum. The solid residue was washed with chilled absolute ethanol followed by diethyl ether and dried under vacuum to recover the product (yield >90%).

##### 4.2.2. General methods for the synthesis of diamines **6** and **7**

Under nitrogen atmosphere, 2 mmol of corresponding bisimines (953.14 mg of **2**; 1153.36 mg of **3**) were added in 20 mL absolute ethanol and the solution was refluxed for 15 min. Excess of  $\text{NaBH}_4$  (12 mmol) added to this in three portions each of 4 mmol after 30 min. The reaction mixture was allowed to reflux further for 13 h and then it was cooled at room temperature. The reaction was quenched by the addition of 5 mL conc. HCl. The reaction mixture was dried under vacuum and the residue was dissolved in 50 mL of aq. HCl (3:7;  $\text{HCl}:\text{H}_2\text{O}$ ). The aqueous layer was washed with  $2 \times 50$  mL of dichloromethane followed by basification using the aqueous NaOH solution to pH = 8–10. The compound was extracted with dichloromethane and an organic layer was dried over anhydrous  $\text{Na}_2\text{SO}_4$ ; solvent was evaporated under vacuum to recover products. Compounds were purified by column chromatography using neutral alumina and 3:1 ethyl acetate and *n*-hexane solvent mixture as eluent.

#### 4.3. In-vitro cytotoxic study

##### 4.3.1. Cell line and culture

The IMR 32 and Hep 3B cell lines were obtained from the National Chemical Sciences, Pune whereas Dubecoos Modified Essential Medium (DMEM), Foetus Bovine Serum (FBS) and cisplatin were obtained from HiMedia. The human cell lines IMR 32 and Hep 3B were established in DMEM with 10% FBS in humidified atmosphere supplied with 5%  $\text{CO}_2$  at 37  $^\circ\text{C}$ . The IMR 32 cell line was differentiated as a neuron by using sodium butyrate for 9 days of incubation at 37  $^\circ\text{C}$  in a concentration of 5%  $\text{CO}_2$ . Both the cell lines were utilized to examine the antitumor activity of testing compound at varying concentration.

##### 4.3.2. MTT assay for cell viability/proliferation

The cell growth inhibition was determined by MTT assay with some modifications. Cisplatin and derivatives were dissolved in DMSO and then diluted with water. The content of DMSO in each sample was 1%. Cells were seeded in 96-well plates at a density of  $1 \times 10^3$  cells per well. After incubation for 24 h, the media were removed and the cells were incubated with 20  $\mu\text{L}$  of media containing 5 mg/mL stock solution of MTT in PBS and 60  $\mu\text{L}$  of DMEM and the cells were treated with different concentrations of derivatives of 4,4'-diaminodiphenyl ether. The positive control cells were treated with culture medium containing cisplatin. Finally the culture was incubated for 6 h at 37  $^\circ\text{C}$  in 5%  $\text{CO}_2$  incubator. The resultant formazan crystal formed by metabolically viable cells was dissolved by adding DMSO. The optical density was measured at 570 nm by ELISA reader (METERTech-Σ960). The number of viable cells was proportional to the extent of formazan production.



#### 4.3.3. Statistical analysis for determination of $IC_{50}$

Six duplicates of each sample were screened and obtained data was analyzed in OriginPro 8 for standard error and probit analysis. The percent cytotoxicity index (% CI) was as follows:

$$\%CI = [1 - (OD \text{ of treated cells}/OD \text{ of control cells})] \times 100\%$$

where, CI = cytotoxicity index, OD = optical density.

A plot of % CI versus concentration was obtained from the experimental data for each set of experiments. The values of  $IC_{50}$  (50% growth inhibition of cell) were determined from the graph. Each test was repeated at least three times and the results were expressed as mean  $IC_{50} \pm SD$ .

#### 4.3.4. DNA ladder assay

DNA fragmentation by compounds **2**, **5** and cisplatin were investigated by agarose gel electrophoresis of extracted genomic DNA from treated cell lines. Briefly, exponentially growing cells ( $5 \times 10^6$  cells/mL) were plated in 6-well plates and then incubated for 6 h with compounds **2**, **5** and cisplatin at their  $IC_{50}$  concentrations. These cells were harvested and then lysed in lysis buffer with 0.5% SDS and proteinase K (20  $\mu$ g/mL) for 4 h at 50 °C. The cell lysates were first extracted with tris saturated phenol, phenol:chloroform:isoamyl alcohol (25:24:1, v/v/v) followed by extraction with chloroform:isoamyl alcohol (24:1). The cell lysates were allowed to precipitate at –20 °C for overnight using absolute ethanol containing 0.3 M sodium acetate and recovered by centrifugation. Finally, electrophoresis of the obtained DNA was carried out in 1.4% agarose gel containing ethidium bromide at 40 V for 2–3 h. The gel was examined and photographed under GeNei GelDoc system to visualize intra-nucleosomal DNA fragmentation (laddering).

#### Acknowledgments

VKS acknowledges CSIR, New Delhi, India for the financial support (Project No. 01/2733/13/EMR-II). One of the authors, R. Kadu acknowledges UGC, New Delhi, India for the financial support in the form of fellowship.

#### Appendix A. Supplementary data

Supplementary data related to this article can be found at <http://dx.doi.org/10.1016/j.ejmech.2013.12.035>.

#### References

- [1] H.Z. Zhang, S. Kasibhatla, J. Kuemmerle, W. Kemnitzer, K. Ollis-Mason, L. Qiu, C. Crogan-Grundy, B. Tseng, J. Drewe, S.X. Cai, Discovery and structure–activity relationship of 3-aryl-5-aryl-1,2,4-oxadiazoles as a new series of apoptosis inducers and potential anticancer agents, *J. Med. Chem.* 48 (2005) 5215–5223.
- [2] M.P. Mattson, Apoptotic and anti-apoptotic synaptic signaling mechanisms, *Brain Pathol.* 10 (2000) 300–312.
- [3] K.W. Bair, R.L. Tuttle, V.C. Knick, M. Cory, D.D. McKee, (1-Pyrenylmethyl)amino alcohols, a new class of antitumor DNA intercalators. Discovery and initial amine side chain structure–activity studies, *J. Med. Chem.* 33 (1990) 2385–2393.
- [4] F.F. Becker, B.K. Banik, Polycyclic aromatic compounds as anticancer agents: synthesis and biological evaluation of some chrysene derivatives, *Bioorg. Med. Chem. Lett.* 8 (1998) 2877–2880.
- [5] K.W. Bair, C.W. Andrews, R.L. Tuttle, V.C. Knick, M. Cory, D.D. McKee, 2-(Arylmethyl)amino]-2-methyl-1,3-propanediol DNA intercalators. An examination of the effects of aromatic ring variation on antitumor activity and DNA binding, *J. Med. Chem.* 34 (1991) 1983–1990.
- [6] A. Kamal, B.A. Kumar, P. Suresh, S.K. Agrawal, G. Chashoo, S.K. Singh, A.K. Saxena, Synthesis of 4 $\beta$ -N-polyaromatic substituted podophyllotoxins: DNA topoisomerase inhibition, anticancer and apoptosis-inducing activities, *Bioorg. Med. Chem.* 18 (2010) 8493–8500.
- [7] (a) A. Kamal, B.A. Kumar, M. Arifuddin, S.G. Dastidar, Synthesis of 4 $\beta$ -amido and 4 $\beta$ -sulphonamido analogues of podophyllotoxin as potential antitumor agents, *Bioorg. Med. Chem.* 11 (2003) 5135–5142; (b) A. Kamal, N.L. Gayatri, D.R. Reddy, P.S.M.M. Reddy, M. Arifuddin, S.G. Dastidar, A.K. Kondapi, M. Rajkumar, Synthesis and biological evaluation of new 4 $\beta$ -anilino-and 4 $\beta$ -imido-substituted podophyllotoxin congeners, *Bioorg. Med. Chem.* 13 (2005) 6218–6225; (c) A. Kamal, E. Laxman, G.B.R. Khanna, P.S.M.M. Reddy, T. Rehana, M. Arifuddin, K. Neelima, A.K. Kondapi, S.G. Dastidar, Design, synthesis, biological evaluation and QSAR studies of novel bisepipodophyllotoxins as cytotoxic agents, *Bioorg. Med. Chem.* 12 (2004) 4197–4202; (d) A. Kamal, B.A. Kumar, M. Arifuddin, S.G. Dastidar, Synthesis and biological activity of new 4 $\beta$ -N-Heteroaryl analogues of podophyllotoxin, *Lett. Drug Des. Discovery* 3 (2006) 205–209; (e) A. Kamal, B.A. Kumar, 4 $\beta$ -amino podophyllotoxin congener as potential anticancer agents and a process for the preparation thereof, Patent WO 2008/136018. (f) A. Kamal, B.A. Kumar, M. Arifuddin, Podophyllotoxin derivatives as antitumor agents, Patent WO 2004/073375. (g) A. Kamal, S. Azeeda, E.V. Bharathi, M.S. Malik, R.V. Shetti, Search for new and novel chemotherapeutics for the treatment of human malignancies, *Mini-Rev. Med. Chem.* 10 (2010) 405–435.
- [8] Z.Q. Wang, Y.H. Kuo, D. Schnur, J.P. Bowen, S.Y. Liu, F.S. Han, Y.C. Cheng, K.H. Lee, Antitumor Agents. 113. New 4 $\beta$ -arylamino derivatives of 4'-O-demethylepipodophyllotoxin and related compounds as potent inhibitors of human DNA topoisomerase II, *J. Med. Chem.* 33 (1990) 2660–2666.
- [9] X.-M. Zhou, Z.-Q. Wang, J.-Y. Chang, H.X. Chen, Y.-C. Cheng, K.-H. Lee, Antitumor agents. 120. New 4-substituted benzylamine and benzyl ether derivatives of 4'-O-demethylepipodophyllotoxin as potent inhibitors of human DNA topoisomerase II, *J. Med. Chem.* 34 (1991) 3346–3350.
- [10] Z. Xiao, Y.-D. Xiao, J. Feng, A. Golbraikh, A. Tropsha, K.-H. Lee, Antitumor Agents. 213. Modeling of epipodophyllotoxin derivatives using variable selection k nearest neighbor QSAR method, *J. Med. Chem.* 45 (2002) 2294–2309.
- [11] D.S. VanVilet, Y. Tachibana, K.F. Bastow, E.-S. Huang, K.-H. Lee, Antitumor agents. 207. Design, synthesis and biological testing of 4 $\beta$ -anilino-2-fluoro-4'-demethylpodophyllotoxin analogues as cytotoxic and antiviral agents, *J. Med. Chem.* 44 (2001) 1422–1428.
- [12] K. Tanaka, T. Ino, T. Sawahata, S. Marui, H. Igaki, H. Yashima, Mutagenicity of N-acetyl and N,N'-diacetyl derivatives of 3 aromatic amines used as epoxy-resin hardeners, *Mutat. Res.* 143 (1985) 11–15.
- [13] R. Kadu, V.K. Singh, S.K. Verma, P. Raghavaiah, M.M. Shaikh, Effect of substituents on crystal packing of functionalized 4,4'-bis(benzylideneamino) diphenyl ether(s) and their reduced benzyl forms: synthesis, characterization, optical and thermal properties, *J. Mol. Struct.* 1033 (2013) 298–311.
- [14] A. Jarrahpour, E. Ebrahimi, Synthesis of some new mono- and bis-polycyclic aromatic spiro and bis-nonspiro- $\beta$ -lactams, *Molecules* 15 (2010) 515–531.
- [15] R.N. Salvatore, C.H. Yoon, K.W. Jung, Synthesis of secondary amines, *Tetrahedron* 57 (2001) 7785–7811.
- [16] (a) Y. Ding, H.W. Boone, J.D. Anderson, A.B. Padias, H.K. Hall Jr., Poly(arylene amine)s from the reduction of aromatic polyimines, *Macromolecules* 34 (2001) 5457–5462; (b) H.W. Boone, M.A. Bruck, R.B. Bates, A.B. Padias, H.K. Hall Jr., N,N'-Diphenyl-1,4(5)-dimethoxyanthraquinone diimines: "butterfly" inversion of anthraquinone diimines, *J. Org. Chem.* 60 (1995) 5279–5283; (c) J.W. Ledbetter Jr., Infrared spectra of N-aryl imines of o-hydroxybenzaldehyde between 2000 and 1500  $\text{cm}^{-1}$ , *J. Phys. Chem.* 81 (1977) 54–59; (d) M. Largeron, M.-B. Fleury, A biomimetic electrocatalytic system for the atom-economical chemoselective synthesis of secondary amines, *Org. Lett.* 11 (2009) 883–886.
- [17] (a) K.-H. Lee, C.-S. Choi, K.-S. Jeon, Fluorescence tuning using conjugated aromatic imine systems, *J. Photosci.* 9 (2002) 71–74; (b) S.C. Martens, U. Zschieschang, H. Wadepohl, H. Klauk, L.H. Gade, Tetrachlorinated tetraazaperopyrenes (TAPPs): highly fluorescent dyes and semiconductors for air-stable organic n-channel transistors and complementary circuits, *Chem. Eur. J.* 18 (2012) 3498–3509; (c) A.C. Valdés, G.P. -Luis, I.A. Rivero, Parallel synthesis of polystyrene anchored imine sulfide materials: sorption and metal sensing studies, *J. Mex. Chem. Soc.* 51 (2007) 87–95; (d) D. Madrigal, G.P. -Luis, I.A. Rivero, Synthesis and hydrolysis monitoring of sasin-like resin bound imines by fluorescence spectroscopy, *J. Mex. Chem. Soc.* 50 (2006) 175–179.
- [18] H. Liu, B. Li, D. Liu, Z. Xu, Photo-physical properties of the transition metal ions complexes of the calix[4]arene derivatives, *Chem. Phys. Lett.* 350 (2001) 441–446.
- [19] Y. Mizobe, T. Hinoue, A. Yamamoto, I. Hisaki, M. Miyata, Y. Hasegawa, N. Tohnai, Systematic investigation of molecular arrangements and solid-state fluorescence properties on salts of anthracene-2,6-disulfonic acid with aliphatic primary amines, *Chem. Eur. J.* 15 (2009) 8175–8184 and the references cited in.
- [20] J. Manosroi, P. Dhumtanom, A. Manosroi, Anti-proliferative activity of essential oil extracted from Thai medicinal plants on KB and P388 cell lines, *Cancer Lett.* 235 (2006) 114–120.
- [21] J.-Y. Je, Y.-S. Cho, S.-K. Kim, Cytotoxic activities of water-soluble chitosan derivatives with different degree of deacetylation, *Bioorg. Med. Chem. Lett.* 16 (2006) 2122–2126.
- [22] A.G. Basnakan, S.J. James, A rapid and sensitive assay for the detection of DNA fragmentation during early phases of apoptosis, *Nucleic Acids Res.* 22 (1994) 2714–2715.
- [23] M.M. Ali, S. Sana, Tasneem, K.C. Rajanna, P.K. Saiprakash, Ultrasonically accelerated Vilsmeier hantzsch cyclisation and formylation reactions, *Synth. Commun.* 32 (2002) 1351–1356.